Pergamon

Int. J. Heat Mass Transfer. Vol. 37, No. 3, pp. 485–492, 1994

0017–9310/94 $6.00 + 0.00

Numerical calculation of the transition from subcritical droplet evaporation to supercritical diffusion

FRANK POPLOW†

Fachgebiet Technische Strömungslehre, Technische Hochschule Darmstadt, Petersenstraße 30, D-6100 Darmstadt, Germany

(*Received* 30 *October* 1991 *and in final form* 11 *May* 1993)

Abstract—The unsteady spherically symmetrical evaporation of a cold single-component droplet in atmospheres at pressures above the critical pressure of the liquid and at temperatures above the critical temperature of the liquid is modelled. High pressure phase equilibrium is assumed at the droplet surface, and solubility of the ambient gas in the droplet, temperature and composition inhomogeneities within the droplet, real gas effects and variable property effects are considered. Depending on the ambient conditions, the droplet surface reaches the critical state and vanishes. Thereafter, a pure diffusion problem is treated.

INTRODUCTION

IN MANY combustion systems, cold fuel droplets are introduced into surroundings at temperatures and pressures exceeding the critical values of the fuel. Droplet evaporation under these conditions has been modelled in several theoretical studies. Sánchez-Tarifa *et al.* [1] assumed that there is no discontinuity at the droplet surface, so that subcritical evaporation cannot be represented. Matlosz *et al.* [2] performed a spherically symmetrical boundary layer analysis for a single-component liquid supposing uniform droplet properties and taking into account real gas effects and high pressure phase equilibrium. However, dissolution of ambient gas in the droplet is not considered, which means that for prescribed pressure and droplet temperature, the equilibrium condition for the gaseous component cannot be satisfied. Thus, a droplet's transition to the supercritical state cannot be modelled. In the experimental part of the work, Matlosz *et al.* consider *n*-hexane droplets evaporating in nitrogen atmospheres under high pressures. As in these experiments natural convection has a large influence, unfortunately the results of the present calculations cannot be compared with these experimental results. In a theoretical study, Rosner and Chang [3] investigated spherically symmetrical evaporation in dense atmospheres emphasizing systematical errors associated with the quasi-steady approximation. Temperature and mole fractions within the droplet are assumed to be uniform and time-independent, thus droplet heat-up is not taken into account. However, from the heat balance, Rosner and Chang derived the ambient temperature and pressure conditions under which a droplet can exist at a constant wet bulb temperature and the conditions under which it may attain the critical state. Jin and Borman [4] theoretically investigated quasi-steady high pressure vaporization of multicomponent drops accounting for forced convection and liquid circulation by using empirical correlations for the transport coefficients. Dissolved gas in the liquid is considered in the computation of phase equilibrium, but the computation ignores its diffusion within the droplet. The saturation pressure profile within the droplet is determined, and the results at the droplet surface ($p_{sat} \sim 0.3p$) seem to be inconsistent with the assumption of chemical equilibrium: in this case one expects $p_{sat} = p$. Kadota and Hiroyasu [5] developed a quasi-steady model for high pressure droplet vaporization taking into account natural convection by using empirical correlations. Real gas effects and high pressure phase equilibrium are considered; however, the equilibrium condition for the gaseous component is not satisfied. Kadota and Hiroyasu's theoretical results compare favourably to experiments they had conducted in a previous study. In an asymptotic study, Umemura [6] considers that phase change at supercritical pressures occurs spatially continuously disregarding the fact that at temperatures below the critical temperature, equilibrium between a liquid and a gas phase may well exist even at supercritical pressures. Furthermore, his similarity analysis depends on the assumption that the partial enthalpies per unit mass of all species are the same. Delplanque and Sirignano [7] theoretically investigate evaporation of oxygen droplets in hydrogen atmospheres under high pressures taking into account the most important high-pressure effects. After the droplet surface has reached the critical state, a critical interface with fixed temperature and composition is tracked. It does not seem clear, however, how the

† Present address: BASF Aktiengesellschaft, ZET/EA, L 544, D-6700 Ludwigshafen, Germany.

NOMENCLATURE

A, a, a_i	parameters for equation of state
B, b, b_i	parameters for equation of state
$\vec{d}_i$	driving force for mass diffusion
D_{ij}	diffusion coefficient
H	enthalpy
h	molar enthalpy
h_i	partial molar enthalpy
l	length of element
M_i	molar mass
N, N_i	amount of substance
n, n_i	amount of substance per volume
$\vec{n}$	normal vector
p	pressure
$\vec{q}$, q	heat flux
R	universal gas constant
R_D	droplet radius
R_0	initial droplet radius
T	temperature
t	time
$\vec{u}$, u	velocity
V	molar volume
V_i	partial molar volume
$\vec{V}_i$, V_i	diffusion velocity
x_i	mole fraction
Z	compressibility factor, pV/RT.

Greek symbols

λ	thermal conductivity
μ_i	chemical potential
ρ	density
Φ	dissipation function
Φ_i	fugacity coefficient
ω	acentric factor.

Subscripts

c	critical value
D	droplet
ev	evaporation
i, j, k	referring to species i, j, k
sat	saturation
0	at $t = 0$
∞	at infinity.

Superscripts

L	liquid
V	vapor
Σ	droplet surface.

conditions at this critical interface could be determined in a general multi-component system.

In the present work, an approach to model the transition from subcritical evaporation to supercritical diffusion is presented. Temperature and mole fraction profiles within the droplet and in the atmosphere are calculated as a function of time, and the influence of pressure and ambient temperature is shown. While the droplet heats up, the concentration jump at the phase interface decreases. For sufficiently high pressures and ambient temperatures, this discontinuity eventually completely vanishes. Then, the droplet surface reaches the critical state, and the subcritical droplet evaporation becomes supercritical diffusion. The quality of the results in this study essentially depends on the quality of the equation of state, which plays a central role in the proposed model.

FORMULATION OF THE PROBLEM AND ASSUMPTIONS

At $t = 0$, a droplet with uniform temperature $T = T_{D0}$ and uniform composition $x_i = x_{i0}$ is introduced into a quiescent gaseous environment with uniform temperature $T = T_{\infty 0}$. The ambient pressure, which may be time-dependent, is prescribed.

A spherically symmetrical problem is considered, natural or forced convection is not modelled. As the velocities induced by the evaporation process are small compared to the velocity of sound, the pressure is considered uniform in the whole domain [8]. The influence of surface tension on vapor pressure, which is small for pressures above 1 bar and droplet diameters above 1 μm [8], is neglected. The contribution of viscous dissipation in the energy balance is not considered. Soret and Dufour effects are not taken into account. Mass forces are not involved, and at the phase interface chemical equilibrium is assumed. For both phases as well as for the supercritical state, the Redlich–Kwong equation of state modified by Soave (SRK equation) is used. Using the same equation of state in all three cases, no discontinuity occurs in the model when the droplet surface reaches the critical state.

BASIC EQUATIONS

The basic equations are taken from Hirschfelder *et al.* [9]. The equations of species conservation for a mixture are

$$\frac{\mathrm{D}n_i}{\mathrm{D}t} = -n_i \nabla \cdot \vec{u} - \nabla \cdot (n_i \vec{V}_i), \tag{1}$$

where $\vec{u}$ is the mass average velocity, $\vec{V}_i$ is the diffusion velocity of the ith species, and $\mathrm{D}/\mathrm{D}t$ denotes the material time derivative. $n_i \vec{V}_i$ is calculated with

$$n_i \vec{V}_i = \frac{n^2}{\rho} \sum_j M_j D_{ij} \vec{d}_j, \tag{2}$$

where $\vec{d}_j$ is the driving force for mass diffusion. It involves the derivatives of the chemical potential μ_i when a non-ideal substance is considered:

$$\vec{d}_i = \frac{n_i}{nRT} \sum_{j \neq i} \left(\frac{\partial \mu_i}{\partial x_j} \right)_{T,p,x_k(k \neq i,j)} \nabla x_j. \tag{3}$$

The chemical potential μ_i is calculated from the equation of state.

In the equation of conservation of energy

$$n \frac{\mathrm{D}h}{\mathrm{D}t} = \Phi - \nabla \cdot \vec{q} + \frac{\mathrm{D}p}{\mathrm{D}t} + h \nabla \cdot (\Sigma n_i \vec{V}_i), \tag{4}$$

the heat flux is expressed as

$$\vec{q} = -\lambda \nabla T + \Sigma h_i n_i \vec{V}_i. \tag{5}$$

As the pressure has been assumed uniform, the equation of momentum conservation need not be considered.

At infinity, the boundary conditions $T = T_\infty(p(t))$ and $x_i = x_{i\infty}$ are imposed.

INTERFACE CONDITIONS AT THE DROPLET SURFACE

During the subcritical part of the evaporation process, local chemical equilibrium is assumed at the phase interface. The temperature profile over the interface is continuous, whereas the mole fractions x_i are different on both sides of the droplet surface. At the droplet surface, the following quantities have to be determined:

the mole fractions x_i^{L} and x_i^{V} on the liquid and on the vapor side of the interface,

the interface temperature T^Σ,

and the velocity differences $u^{\mathrm{L}} - u^\Sigma$ and $u^{\mathrm{V}} - u^\Sigma$, where u^Σ is the speed of the droplet surface and u^{L} and u^{V} are the mass average velocities on both sides of the interface.

In a mixture consisting of n species, there are $2n+3$ unknowns which verify the $2n+3$ conditions

of phase equilibrium

$$x_i^{\mathrm{L}} \Phi_i(x_i^{\mathrm{L}}, T^\Sigma, p) - x_i^{\mathrm{V}} \Phi_i(x_i^{\mathrm{V}}, T^\Sigma, p) = 0, \tag{6}$$

of compatibility

$$1 - \Sigma x_i^{\mathrm{L}} = 1 - \Sigma x_i^{\mathrm{V}} = 0, \tag{7}$$

of continuity of mass flux

$$n_i^{\mathrm{L}}(u^{\mathrm{L}} - u^\Sigma + V_i^{\mathrm{L}}) - n_i^{\mathrm{V}}(u^{\mathrm{V}} - u^\Sigma + V_i^{\mathrm{V}}) = 0, \tag{8}$$

and of continuity of heat flux

$$h^{\mathrm{L}} n^{\mathrm{L}}(u^{\mathrm{L}} - u^\Sigma) + q^{\mathrm{L}} - (h^{\mathrm{V}} n^{\mathrm{V}}(u^{\mathrm{V}} - u^\Sigma) + q^{\mathrm{V}}) = 0. \tag{9}$$

In the heat flux condition the enthalpy of vaporization does not appear explicitly. It is contained in the differences of partial enthalpies in both phases.

EQUATION OF STATE

The SRK equation of state for a pure substance is written [10, 3.6.1 ff]

$$p = \frac{RT}{V-b} - \frac{a}{V(V+b)}, \tag{10}$$

where

$$b = 0.08664 \frac{RT_{\mathrm{c}}}{p_{\mathrm{c}}},$$

$$a = a(T) = 0.42748 \frac{R^2 T_{\mathrm{c}}^2}{p_{\mathrm{c}}} \left(1 + f\omega \left(1 - \left[\frac{T}{T_{\mathrm{c}}} \right]^{1/2} \right) \right)^2$$

and

$$f\omega = 0.48 + 1.574\omega - 0.176\omega^2.$$

The critical values T_{c} and p_{c} and the acentric factor ω are found in literature, e.g. in ref. [10].

For mixtures, a and b in (10) are calculated as a function of the pure component values a_i and b_i and of x_i:

$$b = \Sigma x_i b_i$$

and

$$a = \Sigma\Sigma x_i x_j (a_i a_j)^{1/2} (1 - k_{ij}).$$

The interaction coefficients k_{ij} are supposed to be constant. For many mixtures, they can be found in ref. [11].

With the abbreviations

$$Z = \frac{pV}{RT}, \quad A = \frac{ap}{R^2 T^2} \quad \text{and} \quad B = \frac{bp}{RT},$$

(10) is written

$$Z^3 - Z^2 + (A - B - B^2)Z - AB = 0. \tag{11}$$

The fugacity coefficient Φ_i used in the computation of chemical equilibrium is calculated

$$RT \ln \Phi_i = \int_0^p \left(V_i - \frac{RT}{p} \right) \mathrm{d}p, \tag{12}$$

where the partial molar volume is

$$V_i = \left(\frac{\partial VN}{\partial N_i} \right)_{p,T,N_j(j \neq i)}.$$

With the SRK equation, one obtains

$$\ln \Phi_i = \frac{b_i}{b}(Z-1) - \ln(Z-B) + \frac{A}{B}\left(\frac{b_i}{b} - \delta_i \right) \ln\left(1 + \frac{B}{Z} \right), \tag{13}$$

where

$$\delta_i = 2 \frac{a_i^{1/2}}{a} \Sigma x_j a_j^{1/2} (1 - k_{ij}). \tag{14}$$

The derivatives of the chemical potential, which are

needed for the diffusion calculation, are written: $(i \neq j)$

$$\left(\frac{\partial \mu_i}{\partial x_j}\right)_{p,T,x_k(k\neq i,j)} = RT\left(\frac{\partial \ln \Phi_i}{\partial x_j} - \frac{\partial \ln \Phi_i}{\partial x_i} - \frac{1}{x_i}\right). \tag{15}$$

The molar enthalpy $h = h(T, p, x_i)$ and the partial molar enthalpies h_i are derived from ideal gas state values by using departure functions [10, 5.3]. These only depend on the equation of state. This way, specific heat capacities of liquids and vaporization enthalpies need not be determined using separate formulae.

CALCULATION OF MASS DIFFUSION COEFFICIENTS AND THERMAL CONDUCTIVITY

In the case of a binary mixture, the diffusion coefficients D_{12} and D_{21} take the same value equal to the binary diffusion coefficient, and $D_{11} = D_{22} = 0$. In the present calculations, D_{12} for ideal gases is determined using the method of Wilke and Lee for binary gas systems [10, 11.4.1]. As to diffusion of dissolved gas molecules in the liquid and diffusion in the supercritical state, there is considerable uncertainty. For the present calculations, D_{12} for all states is taken to be the ideal gas value multiplied by the compressibility factor Z. This way, a smooth transition between the models for diffusion in the gas, liquid and supercritical state is obtained and the fact that diffusion coefficients in liquids are much lower than in gases is at least qualitatively taken into account.

The thermal conductivity λ for the gaseous, liquid and supercritical states is calculated as proposed by Reid [10].

For reduced densities ρ/ρ_c lower than 2.8, it is evaluated as follows:

1. determination of the dynamic viscosity η_i of each pure component using the Chung correlation [10, 9.4.3],
2. calculation of the thermal conductivity λ_i^0 at low pressures for each pure component using the modified Eucken correlation [10, 10.3.5],
3. finding the low pressure mixture conductivity λ^0 by applying the Wassiljewa mixing law [10, 10.6.1],
4. accounting for high pressure using the method of Stiel and Thodos [10, 10.5.2 ff].

For reduced densities ρ/ρ_c exceeding 2.8, the thermal conductivity of each pure component is determined by the method of Latini *et al.* [10, 10.9.1], and then Li's mixing law [10, 10.12.17 ff] is applied. The influence of pressure is neglected.

Owing to the lack of experimental data, there is considerable doubt in the determination of the transport coefficients at high pressures and high temperatures.

NUMERICAL METHOD

An explicit first order finite volume method is used. As the properties in each element are supposed to be approximately uniform, the droplet surface, which is a surface of discontinuity, must be situated on the boundary between two elements.

For the numerical procedure, the integral form of the conservation equations

$$\frac{\mathrm{D}N_i}{\mathrm{D}t} = -\iint n_i \vec{V}_i \cdot \vec{n}\,\mathrm{d}S \tag{16}$$

$$\frac{\mathrm{D}H}{\mathrm{D}t} = \iiint\left(\Phi + \frac{\mathrm{D}p}{\mathrm{D}t}\right)\mathrm{d}V - \iint \vec{q}\cdot\vec{n}\,\mathrm{d}S \tag{17}$$

is applied to each computational element. The gradients needed to calculate $n_i\vec{V}_i$ and $\vec{q}$ over the element boundaries are assumed to be constant between two neighbor cell centers which are not separated by the surface of discontinuity, or between the cell center and the surface of discontinuity.

The diffusion calculation is Lagrangian. Except for the droplet surface, the calculation of the mass flux and the heat flux across the cell boundaries is straightforward. The determination of the fluxes across the phase interface requires the solution of the system of equations (6)–(9). For the computation of the unknown interface conditions x_i^{L}, x_i^{V}, T^{Σ}, $u^{\mathrm{L}} - u^{\Sigma}$ and $u^{\mathrm{V}} - u^{\Sigma}$, the quantities in the centers of the two elements adjacent to the interface are considered to be given. Then, with a first order approximation of the gradients between the cell centers and the interface, q^{L}, q^{V}, V_i^{L}, $V_i^{\mathrm{V}} = \mathrm{fct}(x_i^{\mathrm{L}}, x_i^{\mathrm{V}}, T^{\Sigma})$ are injected into (8) and (9). The non-linear system can then be solved using a Newton–Raphson procedure. Once x_i^{L}, x_i^{V}, T^{Σ}, $u^{\mathrm{L}} - u^{\Sigma}$ and $u^{\mathrm{V}} - u^{\Sigma}$ are found, the mass fluxes $n_i^{\mathrm{L}}(u^{\mathrm{L}} - u^{\Sigma} + V_i^{\mathrm{L}})$ and the heat flux $h^{\mathrm{L}}n^{\mathrm{L}}(u^{\mathrm{L}} - u^{\Sigma}) + q^{\mathrm{L}}$ across the interface can directly be calculated. After new N_i and H have been computed in all cells, the new temperatures $T = T(h, x_i, p)$ can be found. Now, the volume of each element (and thus the radial positions of all elements) can be determined from the equation of state. Finally, a rezoning procedure assures that the mesh is maintained geometrically similar to the initial one.

In order to avoid a time step restriction due to the explicit treatment of diffusion, a subcycling procedure is used.

COMPUTATIONAL RESULTS

Evaporation of a droplet ($T_{\mathrm{D0}} = 300$ K) consisting of *n*-hexane ($p_c = 30.1$ bar, $T_c = 507.5$ K) in a nitrogen atmosphere is considered. First, time-dependent temperature and mole fraction fields are shown for $p = 100$ bar and $T_\infty = 800$ K. Then, parametrical studies are carried out to show the influence of the ambient conditions on the evaporation process. Finally, evaporation under time-dependent pressure is

studied under thermodynamical conditions typically found in diesel engines.

Under the assumptions made in the present calculations, the evaporation processes of droplets of different initial sizes are all similar. The presentation of the data in Figs. 1–3 is valid for arbitrary values of the initial droplet radius R_0. Calculations of subcritical evaporation are stopped when the droplet radius reaches 5% of its initial value.

EVAPORATION AT $p = 100$ bar AND $T_\infty = 800$ K

Figure 1(a) shows the time evolution of the fuel mole fraction profile. As the droplet heats up, the jump at the interface decreases and finally vanishes at $t/4R_0^2 = 2.13$ s mm^{-2}. The same applies to the jump in $\partial T/\partial r$ at the droplet boundary (Fig. 1(b)). However, zones of high gradients persist after the droplet has got supercritical. Figure 1(c) shows the differences between the mass average velocities u^L and u^V and the velocity u^Σ of the interface. When the droplet surface gets supercritical and the composition on both sides becomes the same, $u^L = u^V$ holds for continuity reasons.

The calculation has been performed with a mesh containing 20 elements of equal length within the droplet. The gaseous element adjacent to the droplet has the length $l_1^V = 0.05 * R_D$, and the length of the mth gaseous element is $l_m^V = 1.2 * l_{m-1}^V$. To test the influence of numerical discretization, the time a droplet gets supercritical is calculated for different meshes and time steps. The original discretization yields $t_{ev}/4R_0^2 = 2.134$ s mm^{-2}, whereas a mesh only half as fine gives $t_{ev}/4R_0^2 = 2.174$ s mm^{-2} (difference 2%). Using the original mesh with a doubled time step, one finds $t_{ev}/4R_0^2 = 2.137$ s mm^{-2}, thus the influence of the time step is negligible.

INFLUENCE OF AMBIENT TEMPERATURE

In Figure 2 the influence of T_∞ on vaporization under $p = 100$ bar is shown. For ambient temperatures exceeding 600 K, the droplets get supercritical before their radius reaches 5% of its initial value. The drop radius at the time the surface reaches the critical state increases with ambient temperature. The initial swelling of the drops is due to heat-up. Figure 2(b) shows faster droplet heat-up for higher ambient temperatures. However, the mean droplet temperature does not attain its highest final values for the highest ambient temperatures because in these cases less time is available to heat the drop's center before its surface reaches the critical state. In Fig. 2(c), the nitrogen mole fractions on both sides of the interface are shown. The upper branch refers to the gas phase and the lower branch to the liquid phase. When both branches meet, the droplet gets super-

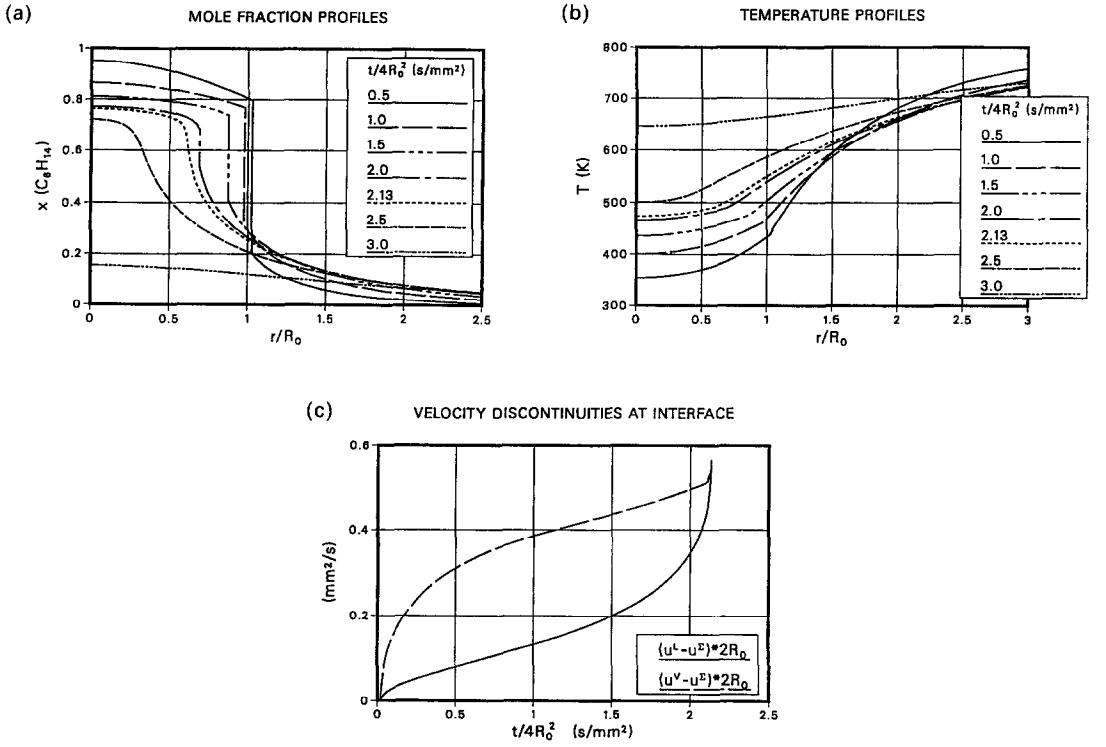

FIG. 1. Calculated fuel mole fraction and temperature profiles and time evolution of the velocity differences at the droplet surface for an n-hexane droplet evaporating in a nitrogen atmosphere at $T_\infty = 800$ K and $p = 100$ bar.

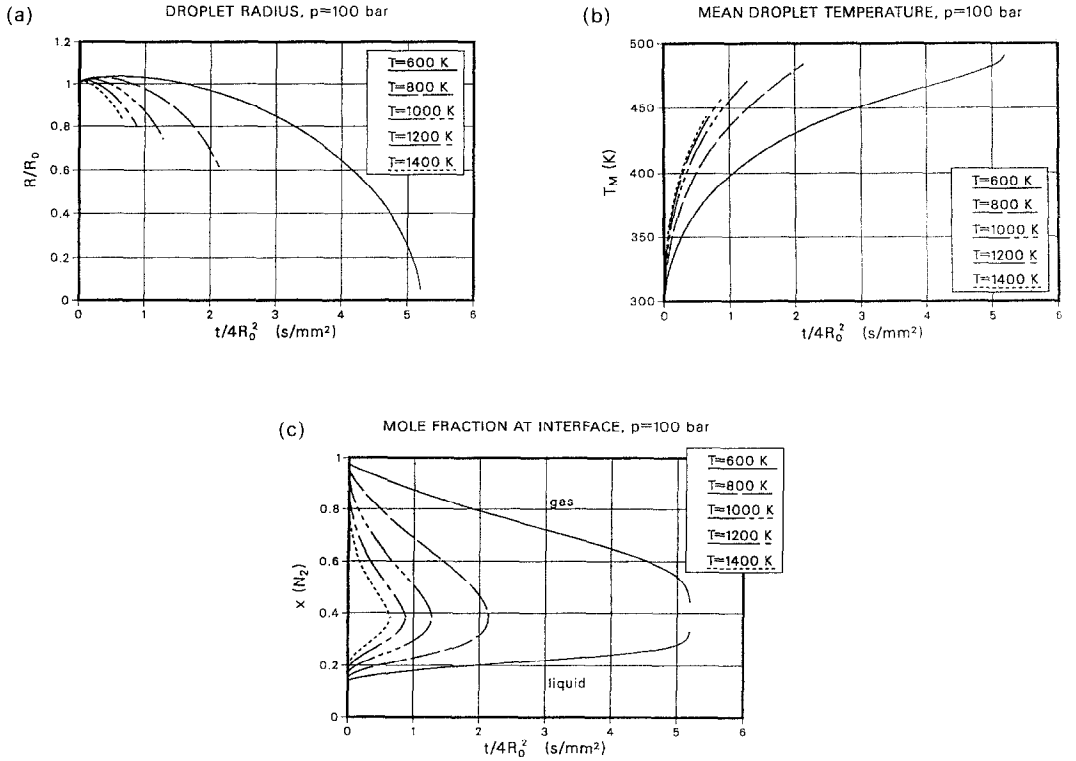

FIG. 2. Calculated radius, average temperature and nitrogen mole fraction histories of *n*-hexane droplets evaporating at $p = 100$ bar in nitrogen atmospheres at different temperatures.

critical. Clearly, under $p = 100$ bar the gas dissolved in the liquid phase should not be neglected.

INFLUENCE OF PRESSURE

In Fig. 3 evaporation in an atmosphere with $T_\infty = 1400$ K is considered under pressures between 40 and 120 bar. Only at $p = 40$ bar, the droplet does not get supercritical before its radius reaches 5% of its starting value; nevertheless, it is far from reaching any constant wet bulb temperature. Increasing pressure causes the droplets to heat up and become supercritical faster. The mean droplet temperature does not reach its maximum values at the highest pressures because, again, the surface reaches the critical state before the interior can be heated. Figure 3(c) shows that the quantity of dissolved gas in the liquid phase grows with increasing pressure.

EVAPORATION UNDER TIME-DEPENDENT PRESSURES

The ambient conditions are chosen to be representative of the thermodynamical conditions found in a diesel engine during the period of fuel injection, if no combustion is supposed to take place. At $t = 0$, the ambient temperature is $T_{\infty 0} = 600$ K, and the pressure is $p = 20$ bar. The pressure changes at a constant rate, until at $t = 1$ ms, $p = 100$ bar is reached. At infinity, an adiabatic compression is supposed to calculate $T_\infty(p(t))$. Initial droplet radii between 6 and 10 μm are considered. Figure 4 shows time evolutions of droplet radius, mean temperature and mole fractions at the surface. The smallest droplet does not get supercritical because it vanishes before the ambient temperature and pressure reach sufficiently high values. The strongly increasing surface regression velocity dR/dt reflects the influence of growing ambient temperature due to compression.

CONCLUSION

A model to simulate spherically symmetrical unsteady droplet evaporation at high pressures considering real gas effects, phase equilibrium and inhomogeneities of temperature and composition in the droplet has been presented. Temperature and concentration profiles show the transition from subcritical evaporation to supercritical diffusion. The influence of ambient temperature and pressure has been shown, and simulations of droplet evaporation at time-dependent pressures typically found in diesel engines have been carried out. Experimental validation is desirable. However, for typical experimental conditions, natural convection is not negligible, and a model taking it into account would be needed.

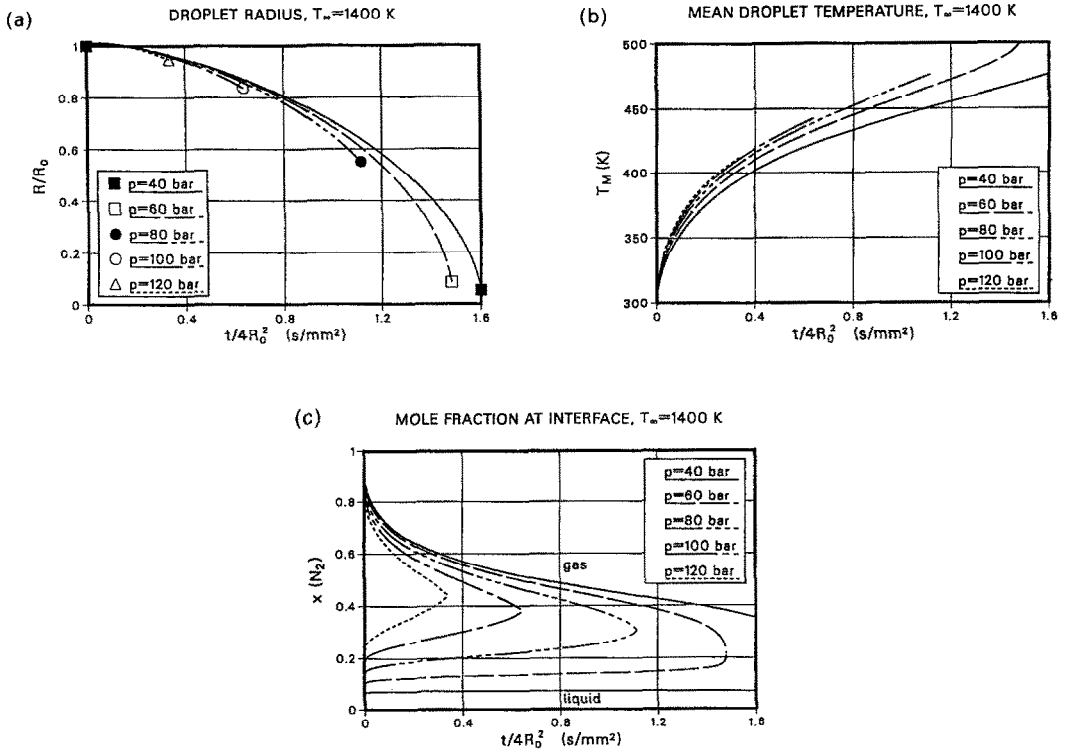

FIG. 3. Calculated radius, average temperature and nitrogen mole fraction histories of *n*-hexane droplets evaporating at different pressures in nitrogen atmospheres at $T_\infty = 1400$ K.

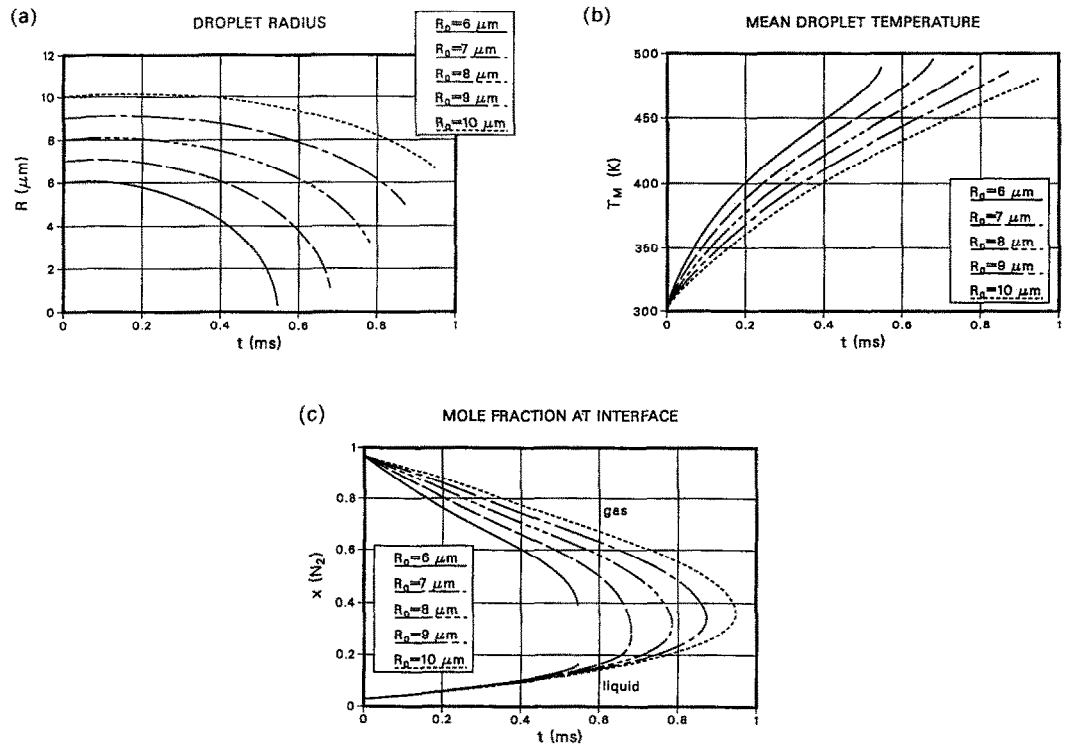

FIG. 4. Calculated radius, average temperature and nitrogen mole fraction histories of *n*-hexane droplets evaporating in a nitrogen atmosphere at $p(t) = 20$ bar $+ 80$ bar $\times (t/1$ ms) and $T_\infty(t = 0) = 600$ K.

REFERENCES

1. C. Sánchez-Tarifa, A. Crespo and E. Fraga, A theoretical model for the combustion of droplets in supercritical conditions and gas pockets, *Acta Astronautica* **17,** 685–692 (1972).
2. R. L. Matlosz, S. Leipziger and T. P. Torda, Investigation of liquid drop evaporation in a high temperature and high pressure environment, *Int. J. Heat Mass Transfer* **15,** 831–852 (1972).
3. D. E. Rosner and W. S. Chang, Transient evaporation and combustion of a fuel droplet near its critical temperature, *Combust. Sci. Technol.* **7,** 145–158 (1973).
4. G. D. Jin and G. L. Borman, A model for multicomponent droplet vaporization at high ambient pressures, SAE paper 850264, *Int. Congress and Exposition*, Detroit, MI, Feb. 25–Mar. 1 (1985).
5. T. Kadota and H. Hiroyasu, Evaporation of a single droplet at elevated pressures and temperatures, *Bulletin JSME* **19**(138) (1976).
6. A. Umemura, The fundamental theory of supercritical evaporation, *Heat Transfer—Jap. Res.* **17,** 82–94 (1988).
7. J.-P. Delplanque and W. A. Sirignano, Numerical study of the transient vaporization of an oxygen droplet at sub- and supercritical conditions, *Int. J. Heat Mass Transfer* **36,** 303–314 (1993).
8. G. M. Faeth, Current status of droplet and liquid combustion, *Prog. Energy Combust. Sci.* **3,** 191–224 (1977).
9. J. O. Hirschfelder, C. F. Curtiss and R. B. Bird, *Molecular Theory of Gases and Liquids*, p. 698. Wiley, New York (1967).
10. R. C. Reid, J. M. Prausnitz and B. E. Poling, *The Properties of Gases and Liquids*. McGraw-Hill, Singapore (1988).
11. D. E. Behrens and R. Eckermann, *Vapor–Liquid Equilibria for Mixtures of Low Boiling Substances*, Vol. 6. DECHEMA, Frankfurt a. M. (1982).